ISPRS Journal of Photogrammetry and Remote Sensing 68 (2012) 1–12

Contents lists available at SciVerse ScienceDirect

ISPRS Journal of Photogrammetry and Remote Sensing

journal homepage: www.elsevier.com/locate/isprsjprs

Comparative evaluation of the Vegetation Dryness Index (VDI), the Temperature Vegetation Dryness Index (TVDI) and the improved TVDI (iTVDI) for water stress detection in semi-arid regions of Iran

Parinaz Rahimzadeh-Bajgiran, Kenji Omasa *, Yo Shimizu

Department of Biological and Environmental Engineering, Graduate School of Agricultural and Life Sciences, The University of Tokyo, 1-1-1 Yayoi, Bunkyo-ku, Tokyo 113-8657, Japan

ARTICLE INFO

Article history:
Received 2 July 2010
Received in revised form 29 October 2011
Accepted 30 October 2011

Keywords:
NDVI
NDII7
Land surface temperature
Semi-arid regions
Water status

ABSTRACT

This study aims at developing appropriate methods to detect water stress in the semi-arid regions of Iran. To do this, the Vegetation Dryness Index (VDI) concept, originally developed for forest fire detection, was applied to detect vegetation/soil water stress. A modified approach towards the Temperature Vegetation Dryness Index (TVDI) concept, incorporating air temperature and a Digital Elevation Model (DEM) to develop the improved TVDI (iTVDI) is also introduced and the results are compared with the original TVDI and VDI through verification by precipitation and soil moisture data. Evaluation of the VDI in the study area showed that there was no significant relationship between the VDI values and precipitation or soil moisture indicating its inappropriateness to be used for water stress detection. Compared with the TVDI, results indicated that there were more statistically significant relationships between the iTVDI and recent precipitation and soil moisture in the four land cover types in the study area. This indicates that the iTVDI is highly influenced by recent precipitation during the summer and can therefore estimate water status. It is concluded that the iTVDI can be successfully used for vegetation/soil water stress monitoring in the semi-arid regions of Iran.

1. Introduction

Semi-arid regions, which are characterized by low and erratic annual precipitation, comprise 61% of Iran. Therefore, vegetation and soil water stress is a major widespread problem in the country. Drought is a common natural disaster, requiring action to monitor and detect water stress, to mitigate its negative impacts on human life, and wildlife and plant communities. Water content in soil and vegetation can be estimated using three different methods: (1) field measurements; (2) meteorological data; and (3) remote sensing. Although field measurements are the most accurate methods for estimating soil and vegetation water content, they are expensive and time consuming especially for mountainous and remote areas. There exist several climatic and hydrological drought indices (point-based) which are based on meteorological data. However, point-based data are often poorly distributed and are insufficient and not available for timely water stress/drought detection. In contrast, remote sensing methods enable us to monitor water stress at higher temporal and spatial resolutions at lower cost and time.

Since the 1980s a number of remote sensing indices have been developed to investigate vegetation condition and amount or soil moisture for drought monitoring. Advanced High Resolution Radiometer (AVHRR) data, supplied by National Oceanic and Atmospheric Administration (NOAA), were the first remotely sensed data used for vegetation condition and changes monitoring providing the ability to generate the NDVI (Normalized Difference Vegetation Index), and the land surface temperature (LST). The NDVI is a common vegetation index reflecting vegetation amount and chlorophyll content and one of the first remotely sensed indices successfully used for monitoring vegetation condition and drought detection at regional scale (Anyamba and Tucker, 2005; Kogan, 1990; Liu et al., 1994; Malo and Nicholson, 1990; Tucker et al., 1981; Vicente-Serrano et al., 2006). However, the NDVI has two main limitations for drought monitoring; first the apparent time lag between rainfall and the NDVI response (Rahimzadeh-Bajgiran et al., 2008, 2009; Rundquist and Harrington, 2000; Wang et al., 2001) and second, little influence of significant precipitation events later in the growing season (plant seed production period) on the NDVI (Rahimzadeh-Bajgiran et al., 2008, 2009; Wang et al., 2001). The NDVI is often referred to as a greenness index which represents the vegetation amount and chlorophyll content of the vegetation rather than water status of the region. Therefore, there

* Corresponding author. Tel.: +81 3 5841 5340; fax: +81 3 5841 8175.
E-mail address: aomasa@mail.ecc.u-tokyo.ac.jp (K. Omasa).

0924-2716/$ - see front matter © 2011 International Society for Photogrammetry and Remote Sensing, Inc. (ISPRS) Published by Elsevier B.V. All rights reserved.
doi:10.1016/j.isprsjprs.2011.10.009

is a need for a more sensitive indicator than the NDVI for water stress monitoring.

To overcome these problems, approaches combining vegetation indices and the LST were proposed for determining canopy water status. The LST is a good indicator of energy partitioning at the surface. In the case of drought, the LST can be used as a proxy for soil and vegetation water stress estimation for the reason that in dry condition due to the lack of soil moisture, both leaf temperature (a result of stomata closure) and surface temperature will increase. Application of the LST for detecting canopy water stress and crop evapotranspiration rate dates back to the 1970s using aerial thermal scanners (Bartholic et al., 1972; Heilman et al., 1976). The earliest applications of thermal scanning techniques and energy balance analysis for plant physiology study on stomata response and transpiration activities at the leaf level were reported in the early 1980s (Hashimoto et al., 1984; Omasa et al., 1981a,b; Omasa and Croxdale, 1991). Later, using remote thermal sensing devices, indices such as the Crop Water Stress Index (CWSI) were developed for irrigation scheduling (Idso et al., 1981; Jackson et al., 1981).

Using concepts such as the CWSI at larger scales (using remotely sensed data) was problematic due to the soil background and mixed pixels. Other approaches were necessary to solve the above mentioned problem (Jones, 2004). One approach, used by Nemani et al. (1993), made use of the fact that the NDVI is an indicator of green vegetation cover within the pixels, and therefore the slope of LST vs. NDVI plot gives a measure of stomata conductance and evapotranspiration. Goetz (1997) reported that there is a negative correlation between the LST and the NDVI and indicted that surface temperature can rise rapidly with water stress. Other researchers developed the concept of the LST vs. NDVI relationship and described the triangular shape of the data falling between the LST and the NDVI axes (Gillies and Carlson, 1995; Gillies et al., 1997; Price, 1990). On the basis of the triangular space, the Temperature Vegetation Dryness Index (TVDI) was developed for soil moisture detection in Senegal (Sandholt et al., 2002). Moran et al. (1994) described the data in the LST vs. vegetation index space as a trapezoid and developed the Water Deficit Index (WDI) based on the CWSI concept for soil and vegetation water deficit. Incorporation of the LST data into drought monitoring procedures for naturally vegetated areas is still a subject for further improvements. A comprehensive review on the application of remotely sensed LST/vegetation indices for the estimation of soil surface moisture and evapotranspiration can be found in Petropoulos et al. (2009) and Li et al. (2009).

Vegetation Water Indices (VWIs) using near infrared wavelengths around 1240, 1640 or 2100 nm in combination with that around 860 nm have been applied as independent vegetation measures for retrieving canopy water content (Tucker, 1980). VWIs are considered to provide us with valuable information on vegetation and/or soil water status and detecting drought. According to these concepts, the NDII (Normalized Difference Infrared Index) using 2100 and 860 nm wavelengths (Hardisky et al., 1983) or using 1600 and 860 nm wavelengths (Hunt and Rock, 1989) was proposed to retrieve land surface moisture condition. Gao (1996) introduced the Normalized Difference Water Index (NDWI) using 1240 and 860 nm wavelengths to retrieve vegetation water content. A similar formula to that of the NDWI to retrieve the EWT (Equivalent Water Thickness) was applied to shrub steppes, shrub savannahs, tree savannah, and savannah woodlands (Ceccato et al., 2002). Fensholt and Sandholt (2003) developed the Shortwave Infrared Water Stress Index (SIWSI) using 1640 and 860 nm wavelengths and found a strong relationship between the index and soil moisture in semi-arid environment of Sahelian zone in Africa. Cheng et al. (2008) indicated the capability of the MODIS NDWI and NDII (using MODIS band 2 (841–876 nm) and 6 (1628–1652 nm)) to estimate canopy water content in a semi-arid site in Arizona. It seems that the NDWI is more suitable for detecting severe vegetation water stress, whereas the NDII can be used to detect low/moderate water stress more accurately as bands with higher water absorption are used in its calculation.

Many studies have shown that the combination of both the NDVI and VWIs can provide great information on vegetation phenology and types as well as water availability. The main reason for these combinations is that high chlorophyll contents do not necessarily indicate high water contents and vice versa (Huete, 2005). Rather, vegetation indices such as the NDVI and VWIs each provide information on two different aspects of vegetation condition, being chlorophyll amount and water content, respectively. Maki et al. (2004) adopted the concept used by Moran et al. (1994) and developed the Vegetation Dryness Index (VDI) using the SPOT/VEGETATION NDVI and NDWI to estimate fire risk in a forest in Russia. Also MODIS band 2 and band 6 (NDWI) with the NDVI and the Enhanced Vegetation Index (EVI) as a surface moisture index were applied to monitor paddy rice agriculture dynamics (Xiao et al., 2005). Gu et al. (2007) developed the Normalized Difference Drought Index (NDDI) using MODIS NDVI and NDWI (derived from MODIS band 2 and band 7 (2105–2155 nm)) for drought detection in grasslands in Finit Hills ecoregion-USA and reported that the NDDI can detect drought in the study area. However, very limited studies have been conducted and well documented for vegetation and soil water stress detection in arid and semi-arid regions using these indices in combination with vegetation indices such as the NDVI.

In Iran, the AVHRR–NDVI has been employed for drought monitoring and the results have shown its capabilities for drought detection in the studied regions (Rahimzadeh-Bajgiran et al., 2008). Also studies on the MODIS NDVI and NDII6 (using band 2 and band 6) and NDII7 (using band 2 and band 7) anomalies for six years have shown the capability of the NDVI and VWIs for differentiating dry years from normal years in the northwest region of the country (Rahimzadeh-Bajgiran et al., 2009). However, as mentioned earlier, the indices were unable to timely detect changes in water status.

Combined application of the NDVI with the LST or VWIs has not yet been studied in Iran. As both VWIs and the LST contain information on soil and vegetation water status, the application of these indices together with vegetation indices such as the NDVI in drought-prone regions of the country is assumed to be considerably beneficial. High-frequency temporal data of the MODIS instrument provide three appropriate water absorption channels for retrieving canopy water content, and suitable thermal and reflective bands. This offers a great opportunity to apply vegetation indices, VWIs and LST at regional and global scale simultaneously.

In this paper, we try to apply VWIs and the LST together with the NDVI for soil/vegetation water stress detection in a semi-arid region in northwest Iran using MODIS products. Three different approaches will be presented and the results will be compared. First the VDI, originally developed for forest fire detection, will be evaluated for vegetation/soil water stress estimation at a larger scale for rangeland and dry farming land covers. A modified approach towards the TVDI incorporating air temperature and a Digital Elevation Model (DEM) to develop the improved TVDI (iTVDI) will be introduced and the results will be compared with those for the TVDI. This modification is meant to improve the performance of the TVDI in the study area where variation in elevation increases the TVDI uncertainty. Temporal and spatial variations of the VDI, the TVDI and the iTVDI will be studied and finally the results of all indices will be validated by using precipitation and surface soil moisture data.

2. Materials and methods

2.1. Definition of the indices

2.1.1. The Vegetation Dryness Index (VDI)

Maki et al. (2004) interpreted the NDVI vs. NDWI scatter plot to estimate vegetation water deficits. The scatter plots indicate that maximum and minimum water content per unit area (NDWI) are associated with leaf quantity per unit area, approximated by the NDVI. Maki et al. (2004) illustrated that this feature is similar to the WDI presented by Moran et al. (1994). The WDI indirectly estimates Fuel Moisture Content (FMC) per leaf quantity with the surface minus air temperature difference ($Ts - Ta$). The VDI, in contrast, directly estimates FMC per NDVI using the NDWI. Fig. 1a illustrates the theoretical trapezoidal shape and the definition of the limits, i.e. dry and wet edges, used to derive the VDI:

$$\mathrm{VDI} = 1 - (BC/AB) \tag{1}$$

where AB and BC are the distances represented on Fig. 1a, between the dry edge (lower limits of the scatter plot) and wet edge of the trapezoid (upper limits in the scatter plot). Vertices (n) in Fig. 1a are poor vegetation with rich water content ($n = 1$), poor vegetation with poor water content ($n = 2$), rich vegetation with rich water content ($n = 3$) and rich vegetation with poor water content ($n = 4$). The VDI is lower for wet and higher for dry conditions and varies between 0 and 1. Note that to be comparable with the two other indices studied here (the TVDI and the iTVDI), the NDVI is the x axis in Fig. 1a. In this study, the NDII7 was used instead of the NDWI as it uses a more appropriate water absorption band for semi-arid regions (Rahimzadeh-Bajgiran et al., 2009).

2.1.2. The Temperature Vegetation Dryness Index (TVDI)

Evapotranspiration rate has been shown to be a good indicator of the land surface water status and can be theoretically estimated through the surface energy balance equation:

$$Rn = G + H + LE \tag{2}$$

where Rn is the radiation flux, G is the soil heat flux, H is the sensible heat flux, L is the latent heat of vaporization and E is the evapotranspiration. Substituting factors in Eq. (2), the latent heat flux LE can be estimated by the following equation:

$$LE = Rn - G - H = \alpha R_{sw} + \varepsilon(R_{lw} - \sigma Ts^4) - G - \rho c_p(Ts - Ta)/r_a \tag{3}$$

where R_{sw} is the shortwave radiation flux from the environment, α is the absorption coefficient of shortwave radiation of the surface, R_{lw} is the longwave radiation flux from the environment, ε is the emissivity of the longwave radiation of the surface, σ is the Stefan–Boltzmann constant, ρc_p is the volumetric heat capacity, and r_a the aerodynamic resistance to heat transfer (Jones, 1992). Ts and Ta are the surface temperature and the air temperature, respectively. Idso et al. (1981) showed that $Ts - Ta$ was linearly related to Vapour Pressure Deficit (VPD) for well-watered crops.

The key step in the development of methods for estimating evapotranspiration rate was developed by Jackson et al. (1981) who introduced the Crop Water Stress Index (CWSI). The CWSI has been shown to be only applicable for fully vegetated covers, and as mentioned before, its application was problematic for remote sensing data. Later, by using the Jackson et al. (1981) concept, the WDI was developed by Moran et al. (1994). The WDI estimates the ratio of LE/LE_p by using land surface temperature and ambient air temperature and can be used for partially vegetated covers. LE_p is the latent heat flux for potential evapotranspiration rate. The WDI is calculated using Eq. (4):

$$\begin{aligned}\mathrm{WDI} &= 1 - LE/LE_p \\ &= 1 - \left[(Ts - Ta) - (Ts - Ta)_{\max}\right] / \left[(Ts - Ta)_{\min} - (Ts - Ta)_{\max}\right]\end{aligned} \tag{4}$$

where $(Ts - Ta)$ is the surface (soil and canopy) temperature minus air temperature at measuring time, and $(Ts - Ta)_{\min}$ and $(Ts - Ta)_{\max}$ are the minimum and maximum $(Ts - Ta)$, respectively, for the same vegetation index value (for example, the NDVI) in the trapezoid space of the vegetation index vs. $(Ts - Ta)$. WDI needs calibration using Penman–Monteith combined with energy balance equation.

In the WDI model, some inputs required to estimate the vertices of the trapezoid are difficult to assess, for example, the aerodynamic resistance (highly affected by wind speed and plant structure), maximum and minimum canopy resistances (both closely related to stomata closure) and soil heat flux (Mendez-Barroso et al., 2008). Providing these data especially for natural vegetation covers is difficult. Therefore, Sandholt et al. (2002) interpreted the AVHRR LST vs. NDVI relationship in terms of soil moisture and proposed the Temperature Vegetation Dryness Index (TVDI) which is a simplification of the WDI model. In the TVDI method, the study area should be large enough to provide a wide range of NDVI and surface soil moisture conditions. The TVDI is estimated using the following equation:

$$\mathrm{TVDI} = (Ts_{\mathrm{obs}} - Ts_{\min})/(a + b\mathrm{NDVI} - Ts_{\min}) \tag{5}$$

where Ts_{obs} is the observed LST at a given pixel, $Ts_{\min}$ is the minimum LST in the NDVI vs. LST space, defining the wet edge, NDVI is the observed Normalized Difference Vegetation Index and a and b are parameters defining the dry edge, modeled as a linear fit to data ($Ts_{\max} = a + b\mathrm{NDVI}$), where $Ts_{\max}$ is the maximum LST observa-

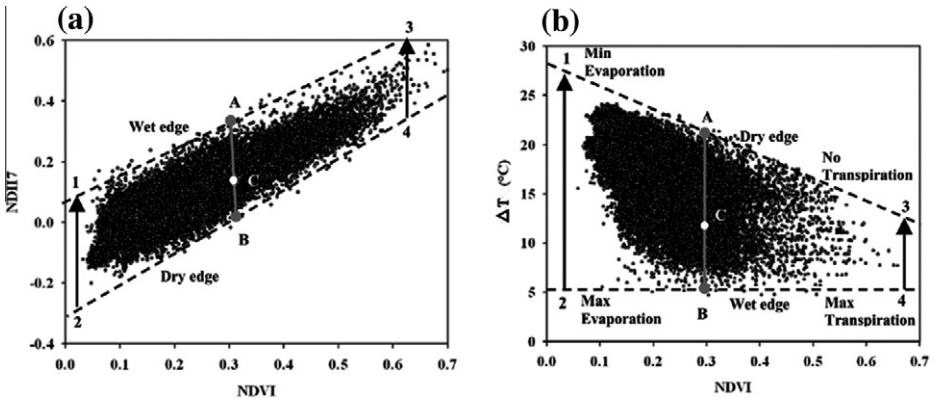

Fig. 1. (a) The trapezoidal shape resulting from the NDII7 vs. NDVI plot to derive the VDI using Method 1, (b) the theoretical trapezoidal shape resulting from ΔT vs. NDVI to derive the iTVDI (location of wet edge and dry edge in scatter plot of ΔT vs. NDVI for DOY 2003-193).

tion for a given NDVI. Parameters *a* and *b* are estimated from an area large enough to represent the entire range of surface moisture content. The TVDI is lower for wet and higher for dry conditions and varies between 0 and 1. Further information on the TVDI calculation can be found in Sandholt et al. (2002).

2.1.3. The improved Temperature Vegetation Dryness Index (iTVDI)

As it is assumed that the main source of variation in the TVDI is soil moisture, air temperature is not considered in the model which may increase the uncertainty of the TVDI for larger areas and higher NDVI values (Sandholt et al., 2002). An inherent assumption when applying the TVDI is that *Ta* is constant for the subset or window over which the index is estimated. A typical error in studies based on the TVDI, is that this assumption is violated in selecting too large an area. On the other hand, when using the TVDI to estimate soil moisture status, heterogeneity of the earth surfaces increases the uncertainty of the TVDI to estimate soil moisture. Therefore, the TVDI should ideally only be applied in regions with little topography. To correct for the effect of topography, Ran et al. (2005) used an approach to correct *Ts* with a DEM before constructing the AVHRR *Ts*/NDVI space. Hassan et al. (2007) proposed a correction method to use a DEM to infer local pressure from altitude and then transform surface temperature to potential temperature.

In this research, we wanted to use the TVDI concept to estimate soil and vegetation water statuses in a mountainous area. Therefore, it seems essential to incorporate air temperature (*Ta*) in the TVDI equation (Idso et al., 1981; Moran et al., 1994) to improve its performance and address the inconsistency in retrieving evaporation and transpiration status (water content status of both low and highly vegetated areas). Using $Ts - Ta$ gradient on the *y*-axis is more physically correct, as it makes the scatter plot of the data more similar to what is described by Moran et al. (1994). The same concept has also been used by Nieto et al. (2010a) for air temperature estimation using remotely sensed data and Nieto et al. (2010b) for dead fuel moisture estimation.

Air temperature decreases as altitude increases, a phenomenon known as the environmental lapse rate. Therefore, a Digital Elevation Model (DEM) of the study area has also been used to calculate the lapse rate to improve the performance of the index to estimate evapotranspiration at different altitudes in each specific month. The new index hereafter called the improved TVDI (iTVDI) is calculated using Eq. (6) and is schematically presented in Fig. 1b.

$$\text{iTVDI} = (\Delta T_{obs} - \Delta T_{min})/(\Delta T_{max} - \Delta T_{min}) = BC/AB \quad (6)$$

where ΔT_{obs} is observed $Ts - Ta$ and *Ta* is observed air temperature calibrated using DEM. ΔT_{min} and ΔT_{max} are the minimum and maximum ΔT, respectively, for the same vegetation index value (here the NDVI). *AB* and *BC* are the distances represented on Fig. 1b, between the dry edge and wet edge in the ΔT vs. NDVI scatter plot as described by Sandholt et al. (2002). Vertices (n) in Fig. 1b are bare soil with no evaporation ($n = 1$), bare soil with max evaporation ($n = 2$), rich vegetation cover with no transpiration ($n = 3$) and rich vegetation with max transpiration ($n = 4$). The iTVDI is lower for wet and higher for dry conditions, and similar to the TVDI, varies between 0 and 1.

In the estimation of the iTVDI from satellite data it is assumed that the trapezoidal scatter plot should be built with thermal data collected over areas experiencing the same thermal inputs, particularly the same net radiation and wind speed. A normalization procedure was suggested by Gillies and Carlson (1995) to correct for variation of net radiation and wind speed. On the other hand, to be determined correctly, the trapezoid of the study area should contain full range of variability in land surface conditions from dry bare soil to saturated bare soil and from water stressed vegetation to well watered vegetation. In this research no correction for effects of topography on net radiation as described by Vincente-Serrano et al. (2004) or daily solar zenith angle variation while using 8-day composite satellite data has been made. Effects of soil and vegetation types on *Ts* and NDVI as mentioned by Lambin and Ehrlich (1996) can also be additional sources of error.

2.2. The study area

The study area covers cold semi-arid regions between 35°N and 37°N latitudes and 47°E and 49°E longitudes in the north-western part of Iran. This area is agriculturally important and contains two protected areas. The area is generally high lands having an altitude of 300–3000 m (Fig. 3a). Mean annual precipitation in this region is around 350 mm, where mean annual temperature is 10.8 °C with the mean maximum and minimum of 18 and 4.5 °C, respectively. The rainy period is generally from November to May, whereas there is almost no precipitation from July to September. The major land cover types in the study area are rangeland, dry farming, and irrigated farming along rivers. The study area also has low to moderate vegetation cover except for irrigated farmlands, and occasional forest and shrubs located in the northern part of the region. Four land cover types including dry farming, plain rangeland, mountainous rangeland, and rangeland and shrubs were selected for analysis in this research (Fig. 2). Detailed information on the characteristics of these land cover types will be presented in Section 3.4.

2.3. Meteorological data

Ambient air temperature from 17 meteorological stations (supplied by Iran Meteorological Organization) for the years of 2000–2005 was used for this research for retrieving $Ts - Ta$ (ΔT) maps. Temperature data were interpolated using the smart interpolation method (Willmott and Matsuura, 1995). For using this method, sixteen Radar Topography Mission (SRTM) DEM images (90 m) of the study area were obtained from Global Land Cover Facilities (GLCF). As considering the general value of the lapse rate (0.6 °C/100 m) is inaccurate and may differ in different places and different months, in this research, environmental lapse rates were calculated using linear regression between air temperature and elevation in each month for available meteorological stations. Lapse rate values calculated for different months in the growing season decreased from 0.48 °C/100 m in April to 0.33 °C/100 m in September. To evaluate interpolation accuracy, a linear regression was performed between estimated and observed temperatures at two stations not included in the interpolation (R^2:0.99). Finally, ΔT maps were produced for each date during summer time for years 2000–2005. Fig. 3 presents the DEM of the study area (a), an example of the interpolated *Ta* map without the DEM incorporation (b), interpolated *Ta* map after the DEM incorporation (c), and corresponding *Ts* map of day 193 of the year 2001 (DOY 2001-193) (d).

Daily and monthly precipitation data for 30 meteorological stations (supplied by Iran Meteorological Organization and Water Resources Research Organization (TAMAB)) in the study area, covering the years 2000–2005 were collected. Precipitation maps were produced using Inverse Distance Weighted (IDW) interpolation method.

2.4. Remote sensing data

For the purpose of this research, MODIS-Terra 8-day, 500-m atmospheric corrected reflectance products (MOD09A1) and 8-day 1000-m land surface temperature products (MOD11A2) for 2000 through 2005, April through September, were obtained to retrieve time series of the VDI, TVDI and iTVDI maps. The images were composites generally located in the middle of each month

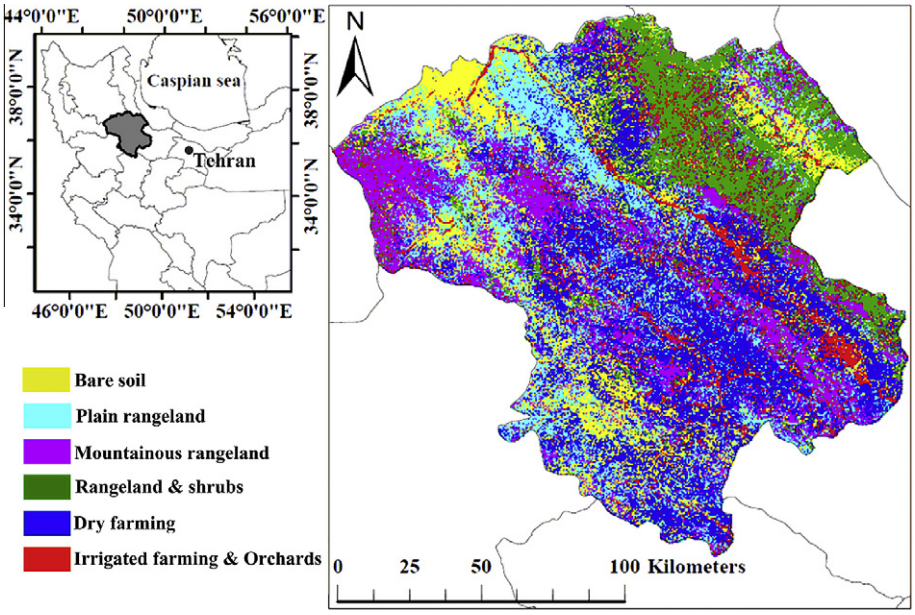

Fig. 2. The location of the study area and the land cover classification map derived from Landsat7/ETM+ images.

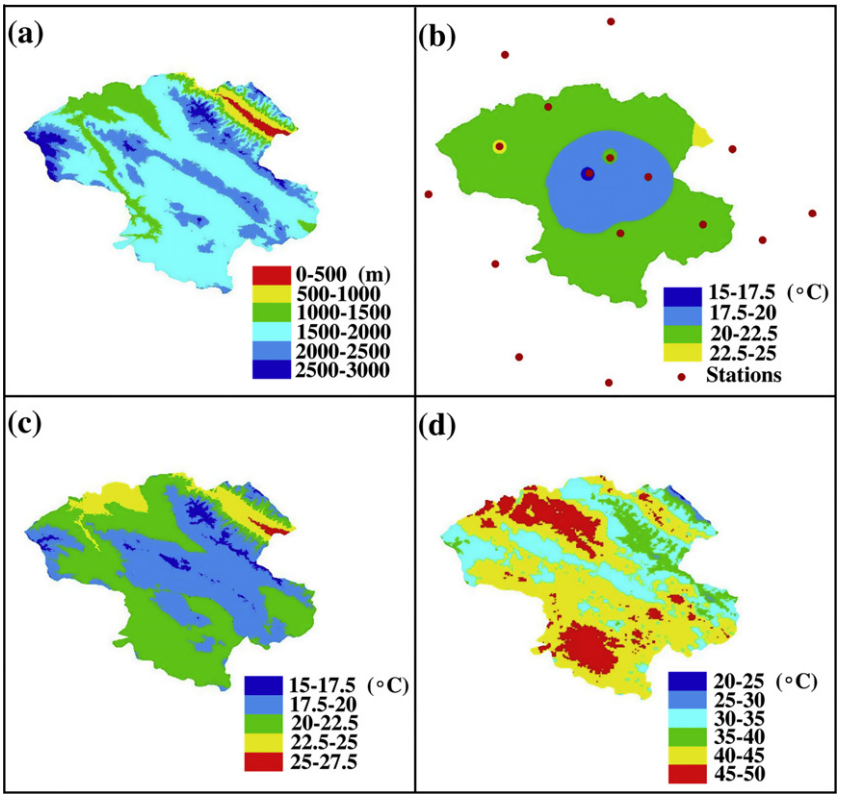

Fig. 3. The DEM of the study area (a), an example of the interpolated *Ta* map without the DEM incorporation (b), interpolated *Ta* map after a DEM incorporation (c), and corresponding *Ts* map (d) of DOY 2001-193.

and were labeled by their DOY starting from the first day of the 8-day period. Daily 500-m atmospheric corrected reflectance product (MOD09GA) and daily 1000-m land surface temperature product (MOD11A1) for 14 August 2008 were used to verify the VDI, TVDI and iTVDI results with measured volumetric soil moisture data. All MODIS products were re-projected using MODIS-MRT tool. Cloud and fill value pixels were masked out using MODIS quality flags data. Pixels with viewing geometry (view/solar zenith angles) values $\leqslant 45^{\circ}$ were used. The 500 m 8-day composite MODIS reflectance product (MOD09A1) was used to derive the NDVI and NDII7 for all six-year data in six months using the following equations:

$$NDVI = (\rho_{NIR} - \rho_{RED})/(\rho_{NIR} + \rho_{RED}) \quad (7)$$

$$NDII7 = (\rho_{NIR} - \rho_{SWIR})/(\rho_{NIR} + \rho_{SWIR}) \quad (8)$$

where ρ_{NIR} and ρ_{RED} are the surface reflectance values of MODIS band 2 (841–876 nm) and band 1 (620–670 nm), respectively, and ρ_{SWIR} is the surface reflectance value of MODIS band 7 (2105–2155 nm) for NDII7. MOD11A2 data contain LST values generated from MODIS data using the generalized split-window LST algorithm (Wan and Dozier, 1996; Wan and Li, 1997). For the purpose of this research, MOD11A2 LST data were resized to 500-m for all six years study period.

To calculate the VDI, wet and dry edges were determined from the scatter plot of the NDII7 and NDVI. Because there was no clear method for the estimation of wet and dry edges, a method similar to that of Verbesselt et al. (2007) was used in this research in two ways. For the first method (herein referred to as Method 1), forty two samples from all natural vegetation covers and bare soil for 6 years during growing season (April through September) were extracted from the NDVI and NDII7 maps. Equations were determined using the NDII7 vs. NDVI plot of the extracted data for the whole study area. For the second method (herein referred to as Method 2), forty two samples were divided into four land cover categories (dry farming, plain rangeland, mountainous rangeland, and rangeland and shrubs) and for each category wet and dry edges were calculated separately. The location of the dry edge and wet edge in the NDII7 vs. NDVI scatter plot for all land covers in the study area (Method 1) is presented in Fig. 1a. The VDI results presented throughout this paper are all derived from Method 1. The reason will be explained in Section 3.1.

The method presented in Sandholt et al. (2002) was used to calculate wet and dry edges for the TVDI using *Ts* vs. NDVI scatter plot. Coefficients of dry edge and wet edge equations were calculated by means of linear regression using the feature space *Ts* vs. NDVI data for each date during the summer time (June–August) in the 6 year study period. These periods are considered water limited periods during growing season. Lack of available moisture content during this period reduces the length of the growing season and decreases plant biomass. For retrieving the iTVDI, the same method as the TVDI was used with the difference that dry edge and wet edge equations were calculated from $\Delta T\,(Ts - Ta)$ vs. NDVI space (Fig. 1b). As the estimation of dry and wet edges can be affected by cloud and noise, care was taken to remove these sources of error.

As the land cover classification map of the study area was available at the coarse resolution, for the purpose of this research, an accurate land cover map was produced using ETM+ data. Four frames of Geocover-orthorectified Landsat 7 products (path and raw: 167/034, 167/035, 166/035 and 166/034) during May and June 2000 were used. As the study area was located in four frames of Landsat7/ETM+ images, in order to have a radiometrically consistent mosaiced image for classification, digital numbers (DN) of all ETM+ imagery were converted to atmospheric corrected reflectance. First, digital numbers of all ETM+ imagery were converted to spectral radiance. Then, using Fast Line-of-Sight Atmospheric Analysis of Hypercubes (FLAASH) atmospheric correction software module, spectral radiances in all ETM+ images were converted to atmospherically corrected reflectance. After atmospheric correction, all images were mosaiced. Different band combinations were studied and finally all bands (except band 6) of ETM+ data were used for classification. Using all bands, differentiation from dry farming and rangelands was more accurate. Training data were collected using field data, Google Earth, ETM+/NDVI map, and ETM+ spectral scatter plots. Maximum likelihood classifications method was used to classify the data. Maximum overall accuracy obtained was 85.05% with a Kappa Coefficient of 0.76 (Fig. 2).

2.5. Fieldwork

A field survey was conducted during 13–15 August 2008 to collect information on vegetation cover types and soil moisture data. Measurements were made in rangelands and harvested dry farming. In each sampling site, four volumetric soil moisture content samples at two depths (5 and 15 cm) were taken using an SM-200 sensor (Delta-T Devices, UK). The soil moisture measuring device is able to measure volumetric soil moisture content with 3% accuracy. Soil samples were also taken for soil physical properties studies and sensor calibration. Field data were used for land cover classification and indices verification.

3. Results and discussion

3.1. Spatial and temporal variation of the VDI, the TVDI and the iTVDI

Spatial and temporal variations of the VDI (calculated using Method 1), the TVDI and the iTVDI for three dates in summer (DOY 161, 193 and 217) during 2001 and 2003 are shown in Fig. 4 through Fig. 6, respectively. During the 2000–2005 study period, year 2001 represents a dry year with around 240 mm annual precipitation whereas year 2003 is considered a normal to slightly wet year having around 350 mm annual precipitation. DOY 161, 193 and 217 are dates during water limited period of the year.

Trends for the VDI images presented in Fig. 4 show that in general, in 2001 and 2003 the VDI maps do not have any particular inter and intra annual dynamics in any of the four studied land cover types. Although years 2001 and 2003 are different regarding water status, the VDI cannot indicate these differences. Even in DOY 2001-161, the VDI values show better water availability (average VDI value 0.53) than DOY 2003-161 (average VDI value 0.57) (average index values are means for the entire study area). In 2003, despite the lack of any precipitation from DOY 161 to DOY 217, the VDI values exhibit an opposite trend, reducing from an average of 0.57 to 0.50. Furthermore, some areas such as mountainous rangeland in the west of the study area (yellow pixels) and dry farming in the north (blue pixels) (see Fig. 2, land cover classification map) show unusual dryness and wetness, respectively in DOY 161, 193 and 217 in both years.

Spatial and temporal variations of the TVDI in the study area (Fig. 5) show that in both 2001 and 2003, DOY 161 had the lowest TVDI values (average values 0.54 and 0.55, respectively) due to April and May rainfalls. In general, DOY 161 in all other years has shown to have lower TVDI values. For DOY 2001-193, the TVDI values (average value 0.62) are higher than DOY 2001-161 due to lack of precipitation. Also for DOY 2003-193, the TVDI values (average value 0.58) are increased because of low rainfall. The TVDI values for DOY 2001-217 decrease (average value 0.56) due to the occurrence of precipitation (between 10 and 50 mm) in July, but for DOY 2003-217, the TVDI values keep rising (average values of 0.60) because of dryness in July. The study of the TVDI in summer time shows that the index values will increase from June to August especially in poor rangeland and dry farming, if there is no precipitation.

Fig. 6 depicts variations in the iTVDI where a similar trend to that of the TVDI can be observed. In both 2001 and 2003, DOY 161 exhibits the lowest iTVDI values (average value 0.56 and 0.54, respectively) as a result of April and May rainfalls. DOY 2003-161 is wetter than 2001-161. In DOY 2001-193 the iTVDI values (average value 0.69) are increased due to lack of precipitation as compared with DOY 2001-161. In DOY 2003-193, because of low rainfall, the iTVDI values (average value 0.64) are higher than DOY 2003-161. In DOY 2001-217, the iTVDI values decrease (average value 0.60) due to the occurrence of precipitation in July, whereas

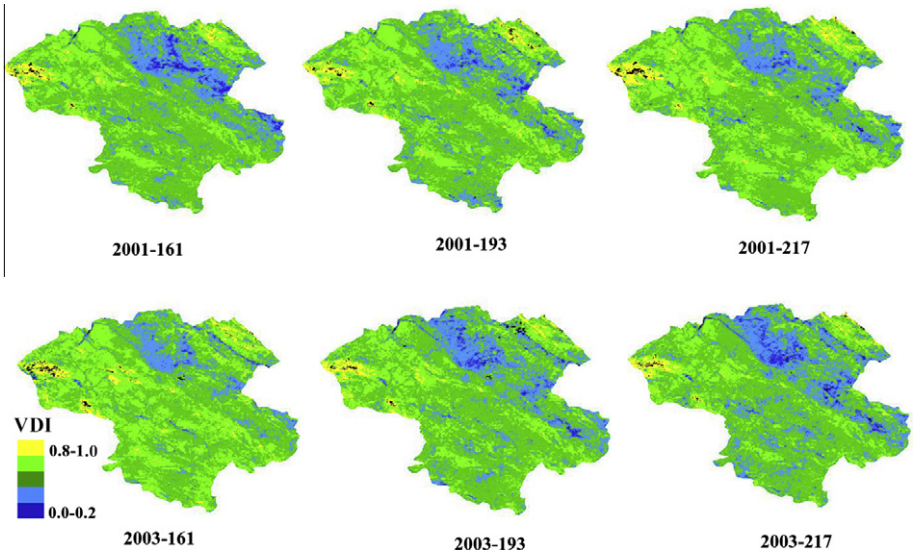

Fig. 4. Spatial and temporal variations of the VDI in DOY 161, DOY 193 and DOY 217 in 2001 and 2003 (black pixels are masked areas due to noise and clouds).

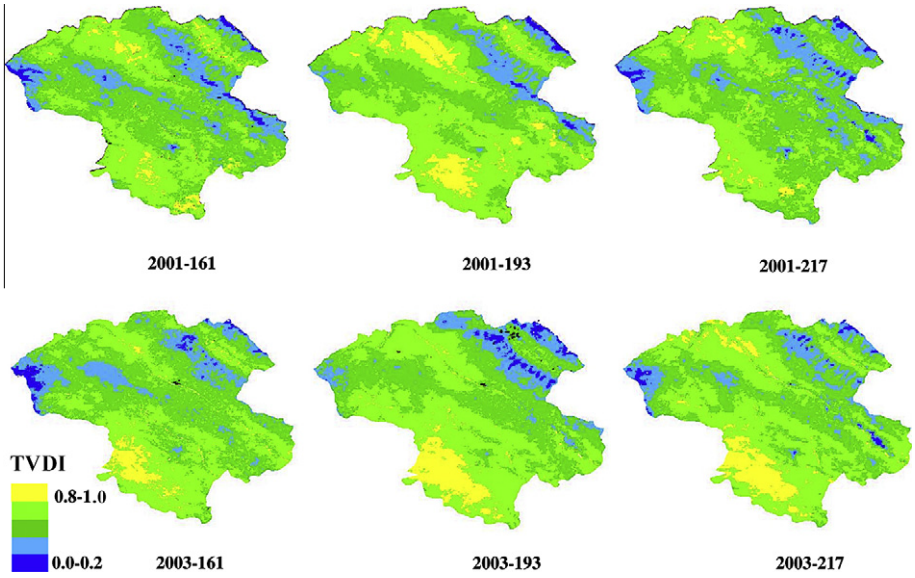

Fig. 5. Spatial and temporal variations of the TVDI in DOY 161, DOY 193 and DOY 217 in 2001 and 2003 (black pixels are masked areas due to noise and clouds).

for DOY 2003-217, the iTVDI values continue to increase (average value 0.67) because of dryness in July. Similar to the TVDI, the iTVDI values will increase from June to August especially in poor rangeland and dry farming, if there is no precipitation. Generally, similar temporal and spatial dynamics can be seen in the TVDI and iTVDI maps. The main difference between the TVDI and iTVDI maps is that the TVDI shows mountainous areas (including mountainous rangeland and rangelands and shrubs) wetter than the iTVDI. Non-mountainous areas on the contrary are shown to have similar index values in both the TVDI and iTVDI maps. Other researchers have also reported similar problems for the TVDI in mountainous areas (Hassan et al., 2007; Ran et al., 2005).

The VDI calculated in this research is expected to show the water deficit for the region from low (bare soil) to high (full vegetation cover) NDVI values (Fig. 1a). Thus, it is expected to provide similar results to those of the TVDI or iTVDI. The VDI quantifies the water content (NDII7) of land surface at a given NDVI value. Studies have shown that the NDII variation is similar to that of the NDVI (Cheng et al., 2008; Rahimzadeh-Bajgiran et al., 2009) and therefore its variation is different from that of Ts or ΔT. In fact, ΔT is an indicator of evapotranspiration rate under constant thermal environments (see Eq. (2)). All land cover types (different NDVI values) can have the same ΔT values according to their water status whereas the NDII7 has seasonal variations making it less responsive to precipitation in the late growing season. On the other hand, the NDII7 is characteristic to each region, and each land cover type has its own range of NDII7 values (Huete, 2005). As a result, the VDI classifies the land covers according to the availability of water content at each NDVI value, and because the ratio of the NDVI to NDII7 in each land cover type stays constant during growing season, the VDI variations cannot be observed. Therefore, blue colored areas in the northern part of the study area (which are dry farming and poor rangeland with better water status than similar areas with the same NDVI values) are always classified as wet areas (VDI = 0.1–0.3) in the VDI maps despite changes during growing season. Also, mountainous rangelands (yellow colored areas in

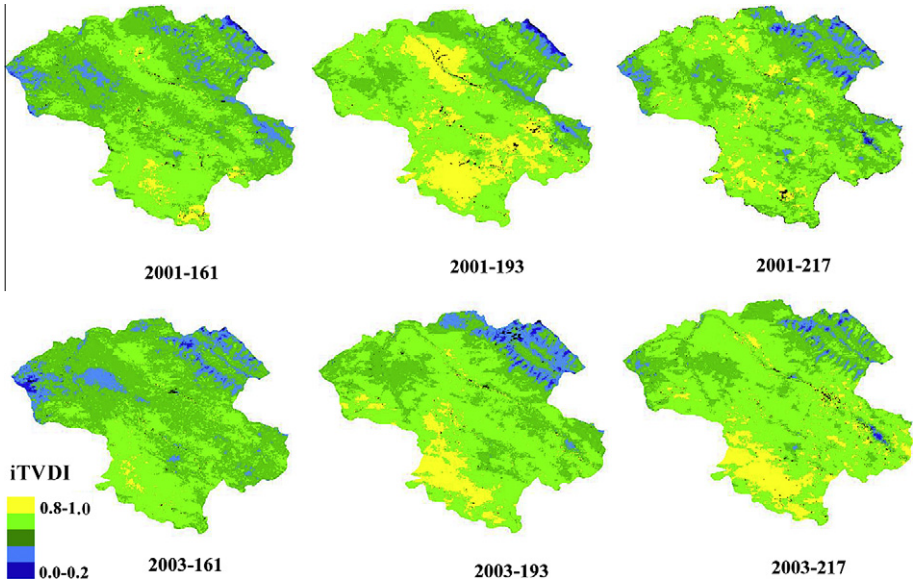

Fig. 6. Spatial and temporal variations of the iTVDI in DOY 161, DOY 193 and DOY217 in 2001 and 2003 (black pixels are masked areas due to noise and clouds).

western part of the study area) which have higher NDVI values are always classified as very dry areas (VDI = 0.7–1). This is due to the characteristics of these areas where the NDII7 values are lower than other areas with the same NDVI values.

To cope with the problem of different NDII7 values in each land cover type in the VDI retrieval, dry and wet edges were also calculated for each land cover type, separately (Method 2). Then, the VDI values were re-calculated for each land cover. Although this resulted in both dry and wet areas in each land cover, on the average, the VDI values were still higher in mountainous areas and lower in dry farming which can be due to the heterogeneity in each land use. Therefore, the problem of unusual wetness or dryness previously observed in Method 1 still persisted in all images. For this reason the results of Method 2 were not presented in this paper. At this stage, working on the improvement of the VDI index was stopped because although finding very homogenous areas would probably improve the performance of the VDI, this would also make the application of the VDI very difficult when applying it at regional scale. On the other hand, application of this index for homogenous areas may be limited to only dense vegetation cover due to the difficulties in using the NDII7 in lower vegetation covers (Fensholt and Sandholt, 2003). As mentioned earlier, considerable fluctuations in the NDII7 values in different land cover types especially those with low to moderate vegetation covers, make it more difficult to use the VDI for such regions.

3.2. Relationships between the VDI, the TVDI, the iTVDI and precipitation

Linear correlation coefficients established between the VDI, the TVDI, the iTVDI and three different precipitation schemes in the four main land cover classes are presented in Table 1. Due to the lack of precipitation in the summer (there was no precipitation within 20 days before each image) the first 30-day cumulative precipitation *before* each image was used as the first precipitation scheme. The two other precipitation schemes were 60-day and 90-day cumulative precipitations. As seen in Table 1, better correlations were established for the iTVDI than the other two indices for all three of the precipitation schemes. No significant relationship was found between the VDI and any of the three precipitation schemes in the study area. Missing values in Table 1 are low positive correlation coefficients between the VDI and precipitation. Compared with the VDI, generally higher coefficients are obtained between the TVDI and precipitation. However, the TVDI was found to have statistically significant relationships with precipitation only in plain rangeland where better correlations were observed when a longer precipitation scheme was used. The coefficients obtained between the iTVDI and precipitation indicate that there are significant relationships between this index and 30-day cumulative precipitation in all land cover types. The relationship between the iTVDI and 30-day cumulative precipitation was strongest for dry farming than for any of the other land cover types.

Fig. 7 presents the anomaly of the VDI, the TVDI and the iTVDI with 30-day cumulative precipitation for the studied land cover types during the summer in 2000–2005. The VDI and precipitation trends are not similar in any of the four land cover types indicating that the VDI is not influenced by recent precipitation. Although trends of the TVDI and the iTVDI are similar to that of precipitation, better agreements are observed for the iTVDI indicating that this index is strongly dependent on rainfall. The TVDI shows less sensitivity to precipitation changes; for example, while in the rangeland and shrubs the iTVDI values change considerably when precipitation occurs, such changes are not reflected in the TVDI values. Comparison of the TVDI and iTVDI values in the studied land cover types shows that the TVDI generally has lower values except for plain rangeland where the values are close to the iTVDI. Also, compared with indices such as the NDVI and VWIs (Cheng et al., 2008; Rahimzadeh-Bajgiran et al., 2008, 2009; Wang et al., 2001), the iTVDI responds to more recent precipitation even in late growing season.

3.3. Relationship between the VDI, the TVDI, the iTVDI and soil moisture

Relationships between the VDI, the TVDI, the iTVDI and precipitation were analyzed in Section 3.2, which implied relationships between the indices and soil moisture or evapotranspiration. As soil moisture database in Iran was not complete, data collected during the August 2008 field survey was used to study relationships with the indices.

As mentioned in Section 2.4, MODIS data for dates of 14 and 15 August 2008 were collected. Due to the severe noise in data on 15

Table 1
Linear correlation results between the VDI, the TVDI, the iTVDI, and three different cumulative precipitation schemes in the four land cover classes during summer 2000–2005.

Land cover types/precipitation	VDI		TVDI		iTVDI	
	R value	*P* value	*R* value	*P* value	*R* value	*P* value
Dry farming						
30-day precipitation	−0.18	0.5396	−0.24	0.4142	−0.84	0.0002
60-day precipitation	–	–	−0.03	0.9120	−0.72	0.0037
90-day precipitation	–	–	−0.22	0.4560	−0.66	0.0144
Plain rangeland						
30-day precipitation	−0.10	0.7167	−0.60	0.0236	−0.77	0.0013
60-day precipitation	−0.03	0.9179	−0.64	0.0138	−0.78	0.0008
90-day precipitation	−0.20	0.5106	−0.74	0.0024	−0.75	0.0029
Mountainous rangeland						
30-day precipitation	–	–	−0.45	0.1049	−0.70	0.0060
60-day precipitation	–	–	−0.21	0.4644	−0.40	0.1597
90-day precipitation	–	–	−0.09	0.7677	−0.17	0.5761
Rangeland and shrubs						
30-day precipitation	−0.06	0.8350	−0.08	0.7980	−0.57	0.0398
60-day precipitation	−0.09	0.7551	−0.02	0.9418	−0.32	0.2638
90-day precipitation	−0.04	0.8793	0.00	0.9933	−0.13	0.6709

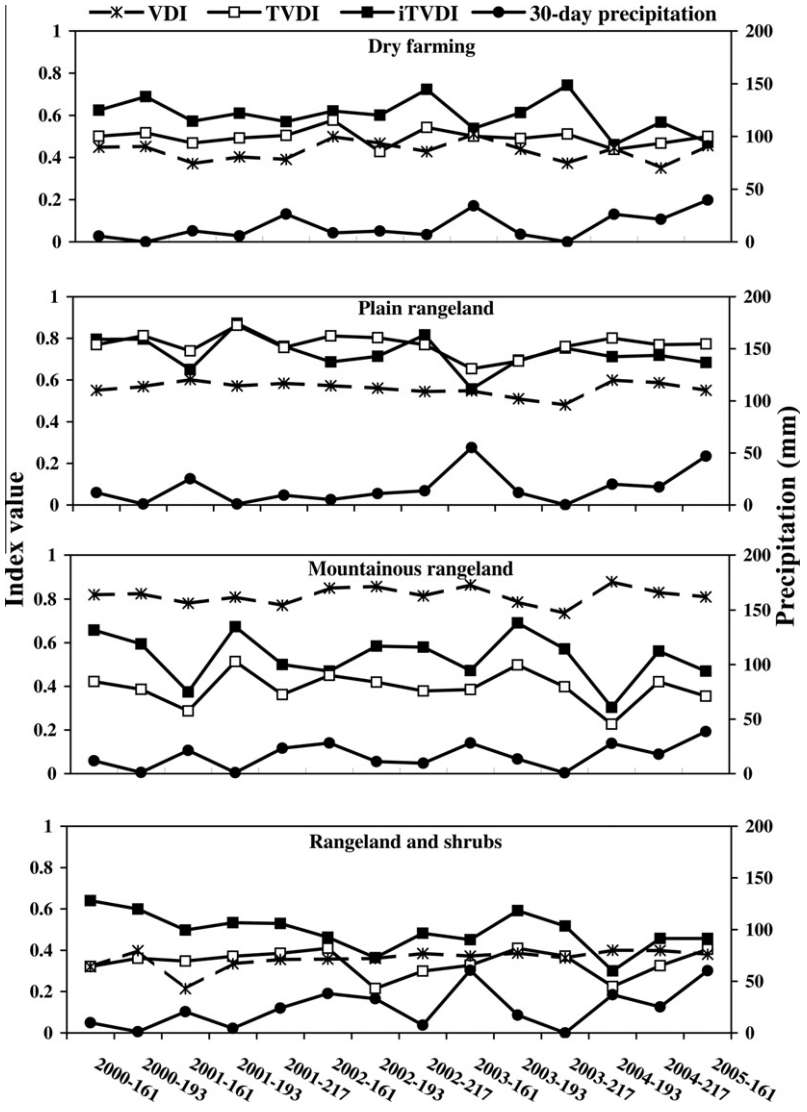

Fig. 7. Anomaly of the VDI, the TVDI, and the iTVDI with 30-day cumulative precipitation in the studied land cover types during the summer in 2000–2005.

August, data for 14 August were used for retrieving the VDI, the TVDI and the iTVDI. Fortunately, air temperature and meteorological conditions were similar on both dates. Year 2008 is considered a dry year with no precipitation occurring during the last 30 days

before the time the images were taken. Soil moisture data were collected from rangelands and dry farming areas at 1200–2200 m elevation. Linear correlations were established between the VDI, the TVDI or the iTVDI, and soil moisture content measured at depths 0–5 and 0–15 cm. The results of the correlations at the depth of 0–5 cm are presented in Fig. 8.

Similar to relationships with precipitation (Section 3.2), the iTVDI was found to have better relationships than the other two indices with soil moisture. No significant relationship was found between soil moisture and the VDI at either depth. Furthermore, as shown in Fig. 8, the relationship between soil moisture and the VDI was found to be positive, whereas the relationships between soil moisture and the TVDI and iTVDI were found to be negative. The relationship between the TVDI and soil moisture showed that there is a significant relationship between them at the depth of 0–5 cm ($R = -0.54$, P value = 0.038) but no significant relationship was found between soil moisture and the TVDI at the depth of 0–15 cm ($R = -0.30$, P value = 0.284). Results show that there were significant relationships between soil moisture and the iTVDI values at both depths, with a stronger relationship at 0–5 cm ($R = -0.80$, P value = 0.0003) than 0–15 cm ($R = -0.67$, P value = 0.006). Comparing the iTVDI values at different elevations showed that using air temperature and environmental lapse rate information can improve the iTVDI performance because areas having similar soil moisture values but at different elevations have similar iTVDI values.

Results for the VDI in this study may not be directly comparable with those from Maki et al. (2004) because, in that study, they verified the VDI results based on SWIR measurement at 1580–1750 nm with pixels of burnt areas in the Russian Far East forests and found that these pixels had comparatively higher VDI values before ignition. However, no verification with soil moisture or fuel moisture content (FMC) was made. On the other hand, Verbesselt et al. (2007) found weak positive relationships while correlating the VDI values based on SWIR measurement at 1580–1750 nm with FMC data in savannah ecosystems and concluded that the NDVI and NDWI still performed better than the VDI. Using a different SWIR wavelength (2100 nm) in this study showed similar weak positive relationships between soil moisture and the VDI values. By modifying the methodology to calculate the VDI, we tried to improve the VDI performance but the results were still unsatisfactory. The VDI cannot be used as a proxy for water stress detection in the study area. Although absorption at 2100 nm might be too strong which can result in saturation, it seems that the VDI failure in the present study can be attributed to other reasons as mentioned in Section 3.1.

As we expected, when using the TVDI to estimate soil moisture status, heterogeneity of the earth surface increases the uncertainty of the TVDI to estimate soil moisture and higher elevated areas will exhibit higher soil moisture content. Although samples taken in the northern part of the study area from rangeland and shrubs had low soil moisture content in the TVDI map, a large part of this area exhibited low TVDI values and appeared to be a no stress area. This has caused weaker relationships between soil moisture and the TVDI in this research. Soil moisture is related to the evapotranspiration rate which is in turn related to ($Ts - Ta$), not solely Ts. Therefore, if Ta is not considered, the estimation will not be accurate. As Ta is not accounted for in the TVDI, this index is less appropriate to indicate water status in the study area, especially when the area is vast and elevation changes greatly.

3.4. Variations of the VDI, the TVDI and the iTVDI in different land cover types

According to the classification map produced using Landsat7/ETM+ data (Fig. 2) and results of the field survey, the major land cover types were rangeland, dry farming, irrigated farming and bare soil. Rangelands in the study area were classified into three categories including plain rangeland, mountainous rangeland, and rangeland and shrubs. Plain rangeland is characterized by low and degraded vegetation covers mostly annual and perennial short grasses including *Agropyron* spp., *Brumus* spp., *Stipa* sp., *Holtemia persica*, *Artemisia* sp., and *Astragalus* sp. located between 1200 and 1700 m in elevation. Mountainous rangeland is less degraded

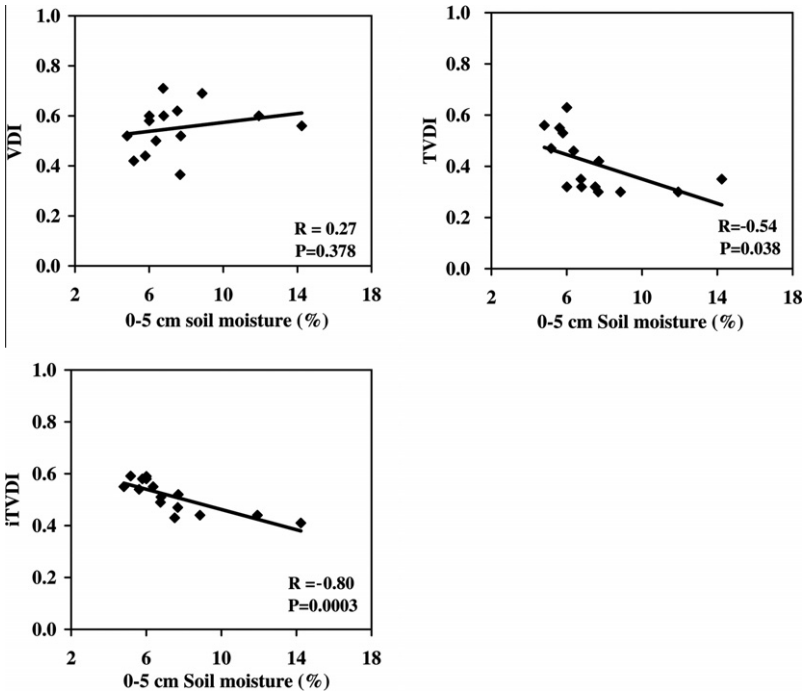

Fig. 8. Linear correlation between the VDI, the TVDI, the iTVDI, and soil moisture content measured at depth of 0–5 cm in August 2008.

and comprised of annual and perennial short grasses and perennials such as *Artemisia* spp., *Festoca* spp., *Bromus* spp., and *Acantholimon* spp. at higher elevations (1700–3000 m). Rangeland and shrubs are also located at higher elevations but vegetation cover compositions are different from plain and mountainous rangeland. This land cover is mostly located in the northern part of the study area and comprised of both grasses, including *Festuca* spp., *Stipa* spp., *Brumus* spp., *Astragalus* spp., and woody shrubs, *Juniperus excelsa*, *Crataegus* spp., *Amygdalus* spp., and *Cotoneaster* sp. at elevations between 1400 and 2700 m.

Plain rangeland and dry farming generally show higher VDI values whereas rangeland and shrubs exhibit lower values but showing no seasonal dynamics (Fig. 4). Three regions display different results; mountainous rangelands which have very high VDI values and poor rangeland and dry farming in the north having low VDI values. As the VDI showed no correlations with precipitation or soil moisture and its spatial and temporal variations were also abnormal, it can be inferred that changes in the VDI values are not dependent on water availability, but rather they are mainly influenced by land cover type.

Comparing the TVDI values and land cover classification map (Figs. 5 and 2) show that the TVDI values are lower in mountainous rangeland and rangeland and shrubs. Although this is a logical trend, because of the poor relationships with precipitation and soil moisture discussed earlier, it can be concluded that TVDI fluctuations are less influenced by water availability.

On the contrary, the iTVDI values were found to be in close agreement with precipitation and soil moisture, therefore it can be inferred that changes in the iTVDI are dependent on the water status in the study area. Comparing the iTVDI values and land cover classification map (Figs. 6 and 2) shows that bare soil, plain rangeland and dry framing always have higher iTVDI values in comparison with mountainous rangeland and rangeland and shrubs in the study area. This can also be easily seen in Fig. 7 where anomalies of the iTVDI in different years are presented. As cumulative precipitation for the growing season was higher in mountainous rangeland and rangeland and shrubs than other land covers, it can be concluded that rangeland and shrubs, mountainous rangeland and dry farming have better water availability, in a descending order, whereas plain rangeland generally suffers from water stress during the summer.

4. Conclusions

In this study, the application of the VDI, the TVDI and the iTVDI for water stress detection in the semi-arid regions of Iran was evaluated and their seasonal and annual variations were studied. The relationships between these indices and precipitation, soil moisture, and land cover types were also analyzed.

Evaluation of the VDI in the study area revealed that this index was more correlated with land cover types, than precipitation or soil moisture. The VDI does not seem to be an appropriate index to detect water stress in the study area. On the other hand, although the TVDI anomalies were in agreement with those of precipitation, it was found to have only significant relationships with precipitation in plain rangeland, whereas, no significant relationships were observed in the three other land covers. The relationship between the TVDI and soil moisture was only significant at the 0–5 cm depth. The iTVDI outperformed the VDI and the TVDI having stronger relationships with precipitation and soil moisture. The iTVDI relationship with recent precipitation in the four studied land cover types was statistically significant and its anomaly was in agreement with precipitation. In addition, strong relationships were observed between the iTVDI values and soil moisture data at both studied depths indicating that this index is a better indicator of instantaneous water status than the two other indices. The application of iTVDI to estimate evapotranspiration and determine water stress in the study area can be recommended.

Theoretically, the iTVDI, the TVDI and the VDI are all expected to estimate water status. The iTVDI was shown to provide better results as compared with the original TVDI when *Ta* and a DEM were introduced into the model. Efforts to obtain satisfactory results for the VDI, even after modifying the approach were in vain. Although absorption at 2100 nm might be too strong, which can result in saturation, it seems that the VDI failure in this study can be attributed to other reasons. In both the VDI and the iTVDI definitions, the NDVI is coupled with the other variable (either NDII7 or ΔT), and therefore, the main reason for their different response to actual water status can be attributed to the *y*-axis response to precipitation or soil moisture. Both ΔT and the NDII7 represent water content of the land cover, but their behaviors are not identical. ΔT variations are a function of irradiation and climatic conditions and are mainly influenced by recent precipitation whereas the NDII7, similar to the NDVI, has seasonal variations making it less responsive to precipitation in the late growing season. Although the NDII7 values are less variable in higher vegetation covers, in lower vegetation covers (NDVI < 0.4), NDII7 values are highly variable in each land cover type with the same NDVI values at any given time. Thus, in the two dimensional space of the NDVI and NDII7 as presented in the VDI definition, the NDII7 value may not be a good representative of water status in low to moderate heterogeneous vegetation covers. Therefore, the VDI does not seem to be applicable to semi-arid heterogeneous regions.

Using ΔT and the NDII7 for water stress detection will provide different information on water status. While ΔT offers information on instantaneous water status, the NDII7 provides information on annual and seasonal dynamics of water status. The NDII7 can differentiate wet and dry years in semi-arid regions and its application in these areas would be beneficial (Rahimzadeh-Bajgiran et al., 2009). However, should the NDII7 be used to determine water status over a time period, it should be incorporated into an index in which its values can be compared with the best conditions at the same pixel level.

References

Anyamba, A., Tucker, C.J., 2005. Analysis of Sahelian vegetation dynamics using NOAA-AVHRR NDVI data from 1981–2003. Journal of Arid Environments 63 (3), 596–614.

Bartholic, J.F., Namken, L.N., Wiegand, C.L., 1972. Aerial thermal scanner to determine temperature of soils and crop canopies differing in water stress. Agronomy Journal 64 (5), 603–608.

Ceccato, P., Flasse, S., Gregorie, J.M., 2002. Designing a spectral index to estimate vegetation water content from remote sensing data: Part 2: Validation and applications. Remote Sensing of Environment 82 (2–3), 198–207.

Cheng, Y.B., Ustin, S.L., Riano, D., Vanderbilt, V.C., 2008. Water content estimation from hyperspectral images and MODIS indexes in Southeastern Arizona. Remote Sensing of Environment 112 (2), 363–374.

Fensholt, R., Sandholt, I., 2003. Derivation of a shortwave infrared water stress index from MODIS near- and shortwave infrared data in a semiarid environment. Remote Sensing of Environment 87 (1), 111–121.

Gao, B.C., 1996. NDWI – a normalized difference water index for remote sensing of vegetation liquid water from space. Remote Sensing of Environment 58 (3), 257–266.

Gillies, R.R., Carlson, T.N., 1995. Thermal remote-sensing of surface soil–water content with partial vegetation cover for incorporation into climate-models. Journal of Applied Meteorology 34 (4), 745–756.

Gillies, R.R., Carlson, T.N., Cui, J., Kustas, W.P., Humes, K.S., 1997. A verification of the 'triangle' method for obtaining surface soil water content and energy fluxes from remote measurements of the Normalized Difference Vegetation Index (NDVI) and surface radiant temperature. International Journal of Remote Sensing 18 (15), 3145–3166.

Goetz, S.J., 1997. Multi-sensor analysis of NDVI, surface temperature and biophysical variables at a mixed grassland site. International Journal of Remote Sensing 18 (1), 71–94.

Gu, Y.X., Brown, J.F., Verdin, J.P., Wardlow, B., 2007. A five-year analysis of MODIS NDVI and NDWI for grassland drought assessment over the central Great Plains

of the United States. Geophysical Research Letters 34, L06407. doi:10.1029/2006GL029127.
Hardisky, M.A., Klemas, V., Smart, R.M., 1983. The influence of soil–salinity, growth form, and leaf moisture on the spectral radiance of Spartina–Alterniflora canopies. Photogrammetric Engineering and Remote Sensing 49 (1), 77–83.
Hashimoto, Y., Ino, T., Kramer, P.J., Naylor, A.W., Strain, B.R., 1984. Dynamic analysis of water stress of sunflower leaves by means of a thermal image processing system. Plant Physiology 76 (1), 266–269.
Hassan, Q.K., Bourque, C.P.A., Meng, F.R., Cox, R.M., 2007. A wetness index using terrain corrected surface temperature and NDVI derived from standard MODIS products: an evaluation of its use in a humid forest dominated region of eastern Canada. Sensors 7 (10), 2028–2048.
Heilman, J.L., Kanemasu, E.T., Rosenberg, N.J., Blad, B.L., 1976. Thermal scanning measurement of canopy temperatures to estimate evapotranspiration. Remote Sensing of Environment 5 (1), 137–145.
Huete, A.R., 2005. Combined land surface water and vegetation indices for land degradation studies in dry land ecosystems. In: Proceedings of Remote Sensing and Geoinformation Processing in the Assessment and Monitoring of Land Degradation and Desertification Conference, Trier, Germany, pp. 398–405.
Hunt Jr., E.R., Rock, B.N., 1989. Detection of changes in leaf water content using near- and middle-infrared reflectances. Remote Sensing of Environment 30 (1), 43–54.
Idso, S.B., Jackson, R.D., Pinter, P.J., Reginato, R.J., Hatfield, J.L., 1981. Normalizing the stress-degree-day parameter for environmental variability. Agricultural Meteorology 24 (1), 45–55.
Jackson, R.D., Idso, S.B., Reginato, R.J., Pinter, P.J., 1981. Canopy temperature as a crop water-stress indicator. Water Resources Research 17 (4), 1133–1138.
Jones, H.G., 1992. Plants and Microclimate: A Quantitative Approach to Environmental Plant Physiology. Cambridge University Press, 428 pp.
Jones, H.G., 2004. Application of thermal imaging and infrared sensing in plant physiology and ecophysiology. In: Advances in Botanical Research Incorporating Advances in Plant Pathology. Academic Press Ltd., London, pp. 107–163.
Kogan, F.N., 1990. Remote-sensing of weather impacts on vegetation in nonhomogeneous areas. International Journal of Remote Sensing 11 (8), 1405–1419.
Lambin, E.F., Ehrlich, D., 1996. The surface temperature–vegetation index space for land cover and land cover-change analysis. International Journal of Remote Sensing 17 (3), 463–487.
Li, Z.L., Tang, R., Wan, Z., Bi, Y., Zhou, C., Tang, B., Yan, G., Zhang, X., 2009. A review of current methodologies for regional evapotranspiration estimation from remotely sensed data. Sensors 9 (5), 3801–3853.
Liu, W.T.H., Massambani, O., Nobre, C.A., 1994. Satellite recorded vegetation response to drought in Brazil. International Journal of Climatology 14 (3), 343–354.
Maki, M., Ishiahra, M., Tamura, M., 2004. Estimation of leaf water status to monitor the risk of forest fires by using remotely sensed data. Remote Sensing of Environment 90 (4), 441–450.
Malo, A.R., Nicholson, S.E., 1990. A study of rainfall and vegetation dynamics in the African Sahel using normalized difference vegetation index. Journal of Arid Environments 19 (1), 1–24.
Mendez-Barroso, L.A., Garatuza-Payan, J., Vivoni, E.R., 2008. Quantifying water stress on wheat using remote sensing in the Yaqui Valley, Sonora, Mexico. Agricultural Water Management 95 (6), 725–736.
Moran, M.S., Clarke, T.R., Inoue, Y., Vidal, A., 1994. Estimating crop water-deficit using the relation between surface–air temperature and spectral vegetation index. Remote Sensing of Environment 49 (3), 246–263.
Nemani, R., Pierce, L., Running, S., Goward, S., 1993. Developing satellite-derived estimates of surface moisture status. Journal of Applied Meteorology 32 (3), 548–557.
Nieto, H., Sandholt, I., Aguado, I., Chuvieco, E., Stisen, S., 2010a. Air temperature estimation with MSG-SEVIRI data: calibration and validation of the TVX algorithm for the Iberian Peninsula. Remote Sensing of Environment 115 (1), 107–116.
Nieto, H., Aguado, I., Chuvieco, E., Sandholt, I., 2010b. Dead fuel moisture estimation with MSG-SEVIRI data. Retrieval of meteorological data for the calculation of the equilibrium moisture content. Agricultural and Forest Meteorology 150 (7–8), 861–870.
Omasa, K., Hashimoto, Y., Aiga, I., 1981a. A quantitative analysis of the relationship between O_3 sorption and its acute effect on plant leaves using image instrumentation. Environmental Control in Biology 19 (3), 85–92.
Omasa, K., Hashimoto, Y., Aiga, I., 1981b. A quantitative analysis of the relationship between SO_2 or NO_2 sorption and their acute effect on plant leaves using image instrumentation. Environmental Control in Biology 19 (2), 59–67.
Omasa, K., Croxdale, J.G., 1991. Image analysis of stomatal movements and gas exchange. In: Hader, D.P. (Ed.), Image Analysis in Biology. CRC Press, pp. 171–193.
Petropoulos, G., Carlson, T.N., Wooster, M.J., Islam, S., 2009. A review of T/WI remote sensing based methods for the retrieval of land surface energy fluxes and soil surface moisture. Progress in Physical Geography 33 (2), 224–250.
Price, J.C., 1990. Using spatial context in satellite data to infer regional scale evapotranspiration. IEEE Transactions on Geoscience and Remote Sensing 28 (5), 940–948.
Rahimzadeh-Bajgiran, P., Darvishsefat, A.A., Khalili, A., Makhdoum, M.F., 2008. Using AVHRR-based vegetation indices for drought monitoring in the Northwest of Iran. Journal of Arid Environments 72 (6), 1086–1096.
Rahimzadeh-Bajgiran, P., Shimizu, Y., Hosoi, F., Omasa, K., 2009. MODIS vegetation and water indices for drought assessment in semi-arid ecosystems of Iran. Journal of Agricultural Meteorology 65 (4), 349–355.
Ran, Q., Zhang, Z., Zhou, Q., Wang, Q., 2005. Soil moisture derivation in China using AVHRR data and analysis of its affecting factors. In: Geoscience and Remote Sensing Symposium, IGARSS '05 Proceedings. IEEE International, pp. 4497–4500.
Rundquist, B.C., Harrington Jr., J.A., 2000. The effects of climatic factors on vegetation dynamics of tallgrass and shortgrass cover. Geocarto International 15 (3), 31–36.
Sandholt, I., Rasmussen, K., Andersen, J., 2002. A simple interpretation of the surface temperature/vegetation index space for assessment of surface moisture status. Remote Sensing of Environment 79 (2–3), 213–224.
Tucker, C.J., 1980. Remote sensing of leaf water content in the near infrared. Remote sensing of Environment 10 (1), 23–32.
Tucker, C.J., Holben, B.N., Elgin, J.H., Mcmurtrey, J.E., 1981. Remote-sensing of total dry-matter accumulation in winter-wheat. Remote Sensing of Environment 11 (3), 171–189.
Verbesselt, J., Somers, B., Lhermitte, S., Jonckheere, I., van Aardt, J., Coppin, P., 2007. Monitoring herbaceous fuel moisture content with SPOT VEGETATION time-series for fire risk prediction in savanna ecosystems. Remote Sensing of Environment 108 (4), 357–368.
Vincente-Serrano, S.M., Pons-Fernandez, X., Cuadrat-Prats, J.M., 2004. Mapping soil moisture in the central Ebro river valley with Landsat and NOAA satellite imagery: a comparison with meteorological data. International Journal of Remote Sensing 25 (20), 4325–4350.
Vicente-Serrano, S.M., Cuadrat-Prats, J.M., Romo, A., 2006. Aridity influence on vegetation patterns in the middle Ebro Valley (Spain): Evaluation by means of AVHRR images and climate interpolation techniques. Journal of Arid Environments 66 (2), 353–375.
Wan, Z.M., Dozier, J., 1996. A generalized split-window algorithm for retrieving land-surface temperature from space. IEEE Transactions on Geoscience and Remote Sensing 34 (4), 892–905.
Wan, Z.M., Li, Z.L., 1997. A physics-based algorithm for retrieving land-surface emissivity and temperature from EOS/MODIS data. IEEE Transactions on Geoscience and Remote Sensing 35 (4), 980–996.
Wang, J., Price, K.P., Rich, P.M., 2001. Spatial patterns of NDVI in response to precipitation and temperature in the central Great Plains. International Journal of Remote Sensing 22 (18), 3827–3844.
Willmott, C.J., Matsuura, K., 1995. Smart interpolation of annually averaged air-temperature in the United-States. Journal of Applied Meteorology 34 (12), 2577–2586.
Xiao, X., Boles, S., Liu, J., Zhuang, D., Frolking, S., Li, C., Salas, W., Moore III, B., 2005. Mapping paddy rice agriculture in southern China using multi-temporal MODIS images. Remote Sensing of Environment 95 (4), 480–492.